Available online at www.sciencedirect.com
ScienceDirect
Journal of Power Sources 174 (2007) 800–804
JOURNAL OF POWER SOURCES
www.elsevier.com/locate/jpowsour

Short communication

Structural and electrochemical characterization of tin-containing graphite compounds used as anodes for Li-ion batteries

A.Trifonova [a,*], M. Winter [b], J.O. Besenhard [b]

[a] *Institute of Electrochemistry and Energy Systems (IEES), Acad. G. Bonchev Street, bl. 10, Bulgarian Academy of Sciences, 1113 Sofia, Bulgaria*
[b] *Institute for Chemical Technology of Inorganic Materials, Stremayrgasse 16, Graz University of Technology, A-8010 Graz, Austria*

Available online 3 July 2007

Abstract

Two tin–graphite composites ("core-shell" structures) with different metal content (80 wt% and 20 wt%) as well as their structural and electrochemical characteristics are presented. Mitsubishi's synthetic carbon was used as starting material for the modification experiments. Chemical reduction was applied for the coating process, which was carried out under inert argon atmosphere. Although a homogeneous film of the nanoscale tin particles (∼60 nm) have been achieved, the electrochemical performance improvement strongly depends on the thickness of the "shell' layer and the progressively increased active surface area together with the tin metal contents. The electrode with low metal concentration displayed both improved cycling performance and stable discharge capacity of 435 Ah kg^{-1} compared with untreated graphite electrode. The tin-rich composite shows a higher medial discharge capacity (540 mAh g^{-1}) but increased capacity fading, while higher metal contents lead to bulk-coated film with disassociated and agglomerated tin nanoparticles as well as higher surface area and likely presence of oxide impurities.

The obtained electrochemical results lead to the assumption, that there is a critical metal ratio up to which good cycling behavior can be achieved. Moreover, the properties of the coating film are closely related with the synthesis conditions and the type of the graphite. In this case, the optimal amount for tin–graphite composite with improved electrochemical performance is about 20 wt%.

Keywords: Tin–graphite composites; Chemical reductive coating; Lithium intercalation; High-density anodes

1. Introduction

The discovery of electrochemical lithium insertion properties of various new materials in recent years and the development of a new generation of high-energy lithium batteries has lead to exploration of Li-storage systems other than the classical negative carbon host ones. Of various carbon materials that have been used, graphite is favored because it has (i) good compatibility with most electrolyte solvents (ii) desirable potential profile for Li-ion intercalation and (iii) also it provides good cycle life and safety and is much cheaper. Unfortunately, the graphite materials are limited by the theoretical specific capacity of 372 Ah kg^{-1} (based on the weight, 339 Ah kg^{-1}, referring to Li_6C), which is rather low compared to the increasingly investigated lithium inserting metals/alloys such as Al, Sn, Si, SnSb, etc. [1–3]. The main shortcoming for all these materials is the volume expansion during the processes of Li insertion/deinsertion, which causes mechanical degradation of the electrode [4,5]. However this problem could be solved when the nanostructured metal, metal oxides and alloys are properly designed. Furthermore, different modifications of graphite such as mild oxidation [6], coating by polymers and other kinds of carbon [7,8], composite formation with metal or alloys [9,10], etc. are also the research activities focus of many scientific groups. For example, Yu et al. [11], report that 10 wt% Ni-coating increases the initial charge–discharge coulomb efficiency of SFG 75 graphite (75 μm, Timcal America) from 59 to 84% and the reversible capacity by 30–40 mAh g^{-1}. In the case of composites of SnSb alloy and MCMB (mesocarbon microbeads), referring to the Popov's group work, when the ratio of SnSb alloy is below 30 wt%, the aggregation of nanosized alloy particles is alleviated, and its cycling behavior is improved with a high stable capacity up to 420 mAh g^{-1} [12]. Other kinds of metals such as Zn and Al [13] can also be coated onto the surface of graphite. The effects are similar to the above-mentioned ones. The objective of our investigations is to combine a high Li-storage capacity of tin (990 Ah kg^{-1} related to $Li_{22}Sn_5$ alloy) together with graphite's good cycleability. Graphite matrix acting as a lithium

* Corresponding author. Tel.: +359 2 979 2728; fax: +359 2 872 2544.
E-mail address: trifonova@bas.bg (A.Trifonova).

0378-7753/$ – see front matter © 2007 Elsevier B.V. All rights reserved.
doi:10.1016/j.jpowsour.2007.06.229

intercalation site and also playing the role of a buffer to the volume expansion of metal is expected.

Tin–graphite composites with different content of metal (80 wt% and 20 wt%) were prepared by chemical reduction process under inert argon atmosphere. The electrochemical performance, structural and morphological design were studied. All investigations were discussed with respect to bare (unmodified) graphite.

2. Experimental

2.1. Synthesis of Sn-coated graphite

Tin encapsulation was carried out via a chemical reduction process at 0 °C under strong stirring and protective argon atmosphere. Prior to the addition of the graphite to the bath for Sn-loading, its surface was cleaned in a mixed aqueous solution containing 20% HCl and 30% NH_5F_2 (ammonium hydrogen difluoride), and heated to 60 °C for 1 h. The solid was then filtered and washed with abundant amounts of decocted de-ionized water, and was added to the bath (300 mL de-ionized water) containing 23.05 mmol sodium citrate as complexant for the metal ions. After 15 min of ultrasonic dispersion, 200 mL Sn^{2+} ion solution (10.0 mmol) was added and the stirring was continued for another 15 min. An alkaline solution (400 mL) of 17.09 mmol $NaBH_4$ in 16.13 mmol NaOH was used as reducing agent. After completion of the reduction process, the obtained tin–graphite composites were separated by filtration and washed thoroughly with dilute HCl, decocted de-ionized water, acetone and dried in vacuum over-night.

Tin–graphite composites with different contents of metal (20 wt% and 80 wt%) were prepared. Changing the concentration of the $SnCl_2$ solution altered the amount of Sn loading.

2.2. Material characterization

The metal amount in the composites was determined using a complexometric (particularly-iodic) analytical method. Each three aliquots from every sample were titrated with a view to data reliability. The following calculated results were obtained: sample I with 20 wt% Sn (19.724 wt%; 19.690 wt%; 19.715 wt%), sample II with 80 wt% Sn (79.803 wt%; 79.791 wt%; 79.840 wt%) respectively.

Gas sorption experiments for defining materials specific surface area were performed with an Autosorb-1 Gas Sorption System (Quantachrome, USA) using N_2 as adsorbant and were interpreted according to the BET theory (Brunauer Emmett–Teller). Particle size distribution of the pristine graphite powder was carried out with a CILAS 1180 particle size analyzer (CILAS, France), operating on the principle of laser diffraction.

The morphologies of the bare and tin-encapsulated graphite were analyzed by scanning electron microscopy. SEM investigations were accomplished with a digital scanning electron microscope (Zeiss DSM 982 Gemini). The phase composition was characterized by X-ray diffraction (XRD) with the use of a D 5005 diffractometer (Siemens, Germany) with Cu Kα radiation.

2.3. Electrochemical measurement

Composite electrodes were prepared by pasting a slurry consisting of 96% (w/o) active materials and 4% (w/o) polyvinylidene fluoride (PVdF) as binder, dissolved in NMP onto a Cu foil with a diameter 12 mm. Further, they were pressed with 20 kg for 10 min and rigorously dried at 120 °C in dynamic vacuum over-night.[1] Electrochemical studies were carried out in "Swagelok" cells with limited electrolyte −1 M L^{-1} $LiPF_6$ (Mitsubishi Chemical Corp.) in EC/DEC (ethylene carbonate/diethyl carbonate, Honeywell, battery grade) with Selgard separator and metallic Li as counter and reference electrodes, applying constant current densities with 0.1 C-rate and setting the cut-off potentials 10–1500 mV versus Li/Li^+. Cell assembly was performed in a glove box under a highly pure, dry argon atmosphere.

Cyclic voltammograms (CVs) were measured at a scan rate of 20 μV s^{-1} using a home build potentiostat, Electrochemical Research Stations Adesys Model 1612 in the same three-electrode cells and the same electrolyte, which was used for the galvanostatic test, between the open circuit voltage (OCV) of the uncharged electrodes and 10 mV as vertex potential.

3. Results and discussions

As mentioned above, a synthetic graphite carbon from Mitsubishi Chemical, which is especially designed as intercalation material for Li-ion batteries, was used. Some preliminary characterizations have been essential. It was found, that this kind of graphite has a smaller specific surface area compared with other graphites $-1.9 \pm 0.2\ m^2\ g^{-1}$. The narrow particle size distribution looks like a Gaussian curve and is given in Fig. 1. There is no small particle size fraction. SE images of the graphite are shown in Fig. 2. The particles have a potato-type shape and a compact structure. The graphite layers exhibit an onionskin-like texture compared with flake-like type as example (SFG), there are no open layers, and loose fragments are nearly absent. From preliminary electrochemical tests it was found that the electrodes start with discharge capacities of 340–350 mAh g^{-1}. However, capacity fading of about 20% for over 35 cycles occurs. The irreversible capacity loss in the first cycle is low and the efficiency is 94%. In the second and subsequent cycles, the difference between charge and discharge capacity decreases rapidly and the coulomb efficiency comes close to 100%.

Fig. 3 displays the XRD patterns of the bare graphite and tin-coated graphite with different contents of metal. The basic peaks of C-substrate and metallic Sn are observed. As can be seen from the graph, the graphite powder is well-graphitized 2H graphite with a strong (0 0 2) diffraction line, d_{002}, which equals 3.35 Å the value of perfect graphite. In the XRD patterns of the composites Sn diffraction lines appear. In the case of high content of Sn a small peak at 25° theta is observed, which

[1] According to the very compact appearance of the particles, see Figs. 1 and 2, the graphite showed an unusual high density, i.e. the slurries were rather small by volume and also had to be painted in thin layers to meet the desired range of active mass.

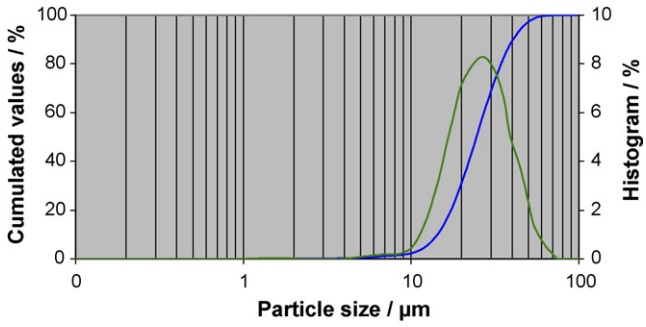

Fig. 1. Particle size distribution of carbon powder

The uncertainty is estimated to be less than ±0.2 μm, it increases for the larger particles up to ±0.5 μm.

Diameter 10%	14.3 μm
Diameter 50%	24.5 μm
Diameter 90%	40.4 μm

Fig. 2. SEM of bare graphite.

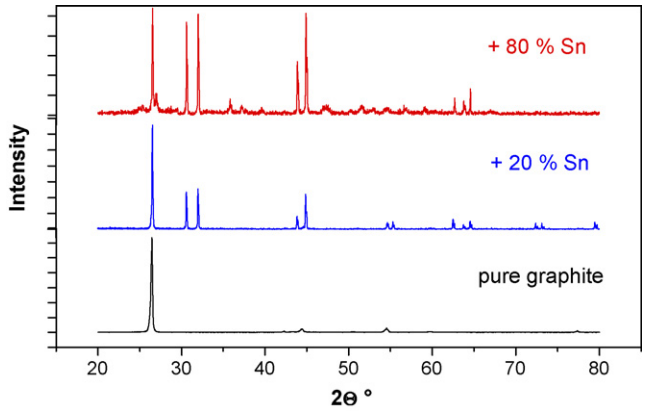

Fig. 3. XRD pattern of the original graphite and the coated powders.

corresponds to $Sn_6O_4(OH)_4$, i.e. surface impurities are present in this sample, which results in the lower first cycle efficiency in galvanostatic cycling and also can clearly be seen in the cyclic voltammograms (see figures below).

Fig. 4 shows SE images of the tin–graphite powders. The amount of disassociated agglomerated tin nanoparticles increases with the content of metal in the composite material. The particle size of the Sn in the composite is reduced to 60 nm (judging from the SEM). Moreover, the dendrite morphology of the pure Sn is not observed in the composites. It is significant that graphite particles provide many active surface-sites for Sn nucleation, so that the metal particles are dispersed on the surface of matrix graphite carbon uniformly and cannot grow adequately to form dendritic structures. The BET surface area was 25.35 $m^2\ g^{-1}$ for the composite with 80 wt% of metal and 3.68 $m^2\ g^{-1}$ for the one with 20 wt% metal. The areas decrease with the particle size, which can be estimated from the SE micrographs. The metallic compounds on the carbon surface will

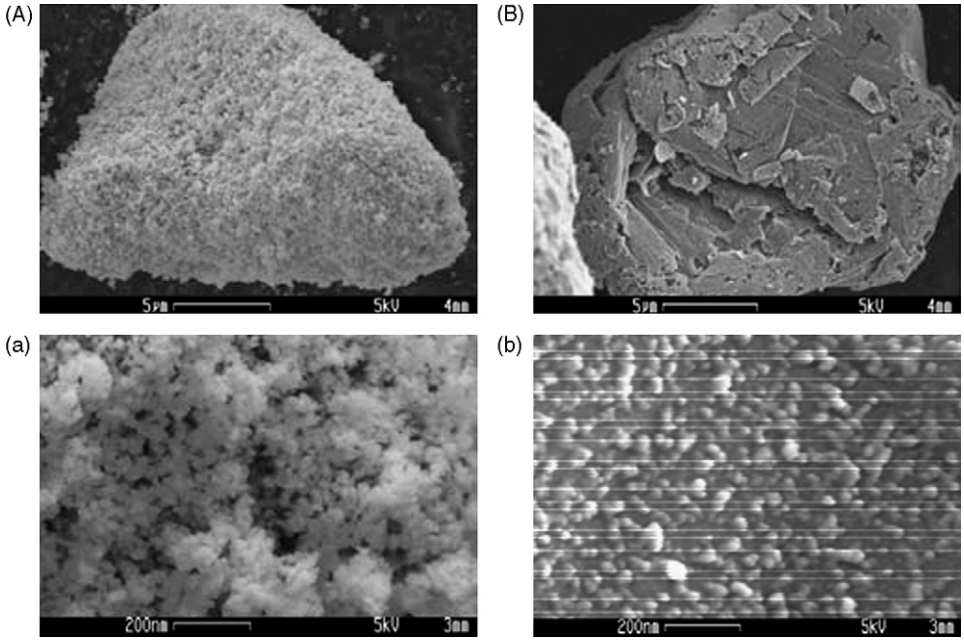

Fig. 4. Scanning electron micrographs of: (A) 80 wt% Sn and (B) 20 wt% Sn. High magnification of the same images: (a) sample (A) and (b) sample (B).

form an artificial SEI film and play the role of an electronically conducting agent in the electrode.

The cyclic voltammograms of the tin–graphite composites as well as of bare graphite are observed in Fig. 5. Four peaks corresponding to four different transitions for the bare graphite electrode are present in the CV curves. The potential region, where most of the lithium insertion occurs, is close to 0.0 V versus the Li/Li^+ reference electrode, whereas the potential for lithium extraction is around 0.2 V. Previously, it was reported [14] that this voltage hysteresis between lithium insertion and extraction might be related to the interstitial carbon atom, especially when the graphite is ball-milled. Our carbon material is, however, a well-graphitized carbon and therefore a different mechanism should be responsible. As shown in Fig. 5(b) and (c), the tin–graphite electrodes show several new reduction and oxidation peaks. These additional redox peaks are related to the participation of elemental Sn to form Li_xSn alloys. The capacity above 0.25 V is mainly attributed to the alloying and de-alloying of Sn. This part provides additional lithium insertion capacity for composite electrodes, in comparison with pure graphite. With increasing of Sn content, the additional reaction peaks become stronger in intensity. In the first CV cycle of sample (c) there is also a peak at around 1.2 V, which can be attributed to the reduction of the surface impurities in the material.

The electrochemical performance of the composites strongly depends of the thickness of the "shell" layer and the progressively increased active surface area together with the contents of tin metal. They are also enhancing lithium kinetics, i.e. they are responsible for the high rate performance. The type of the graphite has a significant role too. The discharge capacities as function of cycle numbers are plotted on Fig. 6(a).

With the increasing of metal content the reversible capacity rises, however, the cycling stability deteriorates. The same problems occur like in pure metal electrodes [15]. The composite electrodes of compounds with higher metal amounts demonstrate a larger irreversible capacity in the first cycle

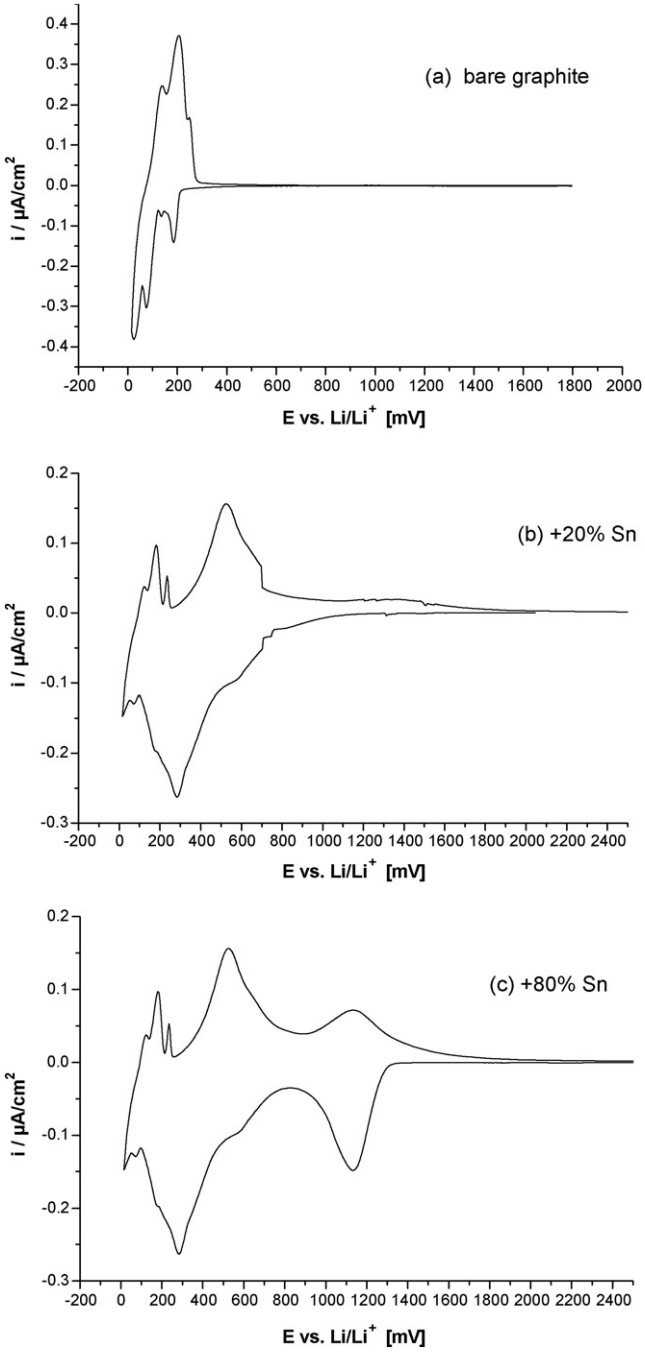

Fig. 5. CVs of (a) bare graphite, (b) 20 wt% tin–graphite and (c) 80 wt% tin–graphite.

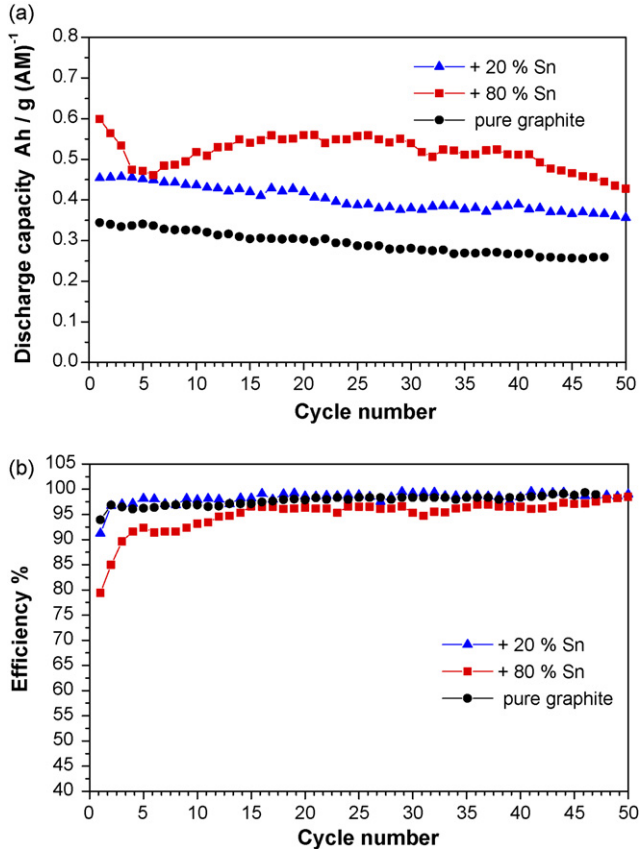

Fig. 6. Lithium insertion capacities (a) and coulombic efficiencies (b) vs. cycle number for graphite and tin–graphite composites.

(Fig. 6(b)) −79% efficiency and poor efficiencies in the first three cycles, even though the medial discharge capacity is about 540 mAh g^{-1}. This can be explained with the higher surface area, the presence of oxide impurities and the bulkiness of the coated film.

In contrast, the material with 20 wt% tin exhibits a much lower irreversible capacity in the first cycle (91% efficiency) and its efficiency reaches almost 99.6% in the consecutive ones. The average discharge capacity is 435 mAh g^{-1} and is stable for more than 50 cycles. In this case, the distance between two metallic particles is far enough to prevent the particle contact after the volume expansion. Such a configuration seems able to reduce the mechanical stress caused by the volume effect and to improve the morphological stability of the composite. Furthermore, the growth of the Sn-grains during prolonged cycling, which then results in problems with the mechanical stability and which was identified as one of the reasons for the poor cycling stability of pure Sn and Sn-based oxides, is prevented, when the single Sn particles are not in contact with each other. This composite electrode presents a good cycling stability. With its small volume expansion for Li accommodation and its elastic structure, the graphite matrix can endure the volume effect of the metallic host and reduce the mechanical stress within the electrode. Lithium insertion and extraction at different voltages corresponds to different active parts in the composites, i.e. at a given voltage only a part of the composite reacts, which again alleviates the whole volume effect and prevents electrode disintegration thus leading to better cycling performance compared with the untreated graphite electrode.

The obtained electrochemical results provide the assumption that there is a critical metal ratio up to which good cycling behavior can be achieved. Moreover, the properties of coating film are closely related to the synthesis conditions and the graphite type. For example, referring to the Yamaki's group work [9], when Sn is supported on large surface-area synthetic graphite (KS6) to obtain composite materials, an improved electrochemical performance relative to bulk Sn is observed. Moreover, when the amount of Sn is adequate, a good cycleability is achieved. In our case, the optimal amount for tin–graphite composite, with improved electrochemical performance is about 20 wt%.

4. Conclusion

Two tin–graphite composites with different metal content (80 wt% and 20 wt%), prepared via chemical reduction under argon atmosphere were investigated. The nano-metal particles (up to 60 nm in size) are dispersed on the C-substrate surface uniformly, indicating that the graphite surface could provide many active sites for Sn nucleation. Dendrite morphology is not observed. The properties of coating film are closely related with the synthesis conditions and the type of the graphite. The composites electrochemical performance improvement strongly depends on the amount of metal coating. Our studies indicate that the best electrochemical behavior is achieved with the material containing about 20 wt% tin metal. This is the optimal amount for good cycling performance.

Acknowledgments

The authors thank Mitsubishi Chemical Corp. (Japan) and Honeywell (Germany) for the donation of samples used in this study.

Dr. Trifonova would also like to specifically acknowledge the financial support of NATO via EAP.RIG.982531.

References

[1] T. Takamura, K. Sumiya, J. Suzuki, C. Yamada, K. Sekine, J. Power Sources 81/82 (1999) 368.
[2] J. Lee, R. Zhang, Z. Liu, J. Power Sources 90 (2000) 70.
[3] A. Trifonova, M. Wachtler, M.R. Wagner, H. Schroettner, Ch. Mitterbauer, F. Hofer, K.-C. Moeller, M. Winter, J.O. Besenhard, Solid State Ionics 168 (2004) 51.
[4] J.O. Besenhard, J. Yang, M. Winter, J. Electrochem. Soc. 68 (1997) 87.
[5] M.M. Thackeray, et al., Electrochem. Commun. 1 (1999) 111.
[6] E. Peled, C. Menachen, J. Electrochem. Soc. 143 (1996) L4.
[7] S. Kuwabata, N. Tsumura, H. Yoneyama, J. Electrochem. Soc. 145 (1998) 1415.
[8] M. Gaberscek, M. Bele, J. Drofenik, S. Pejovnik, J. Power Sources 97/98 (2001) 67.
[9] M. Egashira, H. Takatsuji, S. Okada, J. Yamaki, J. Power Sources 107 (2002) 56.
[10] P. Yu, J.A. Ritter, R.E. White, B.N. Popov, J. Electrochem. Soc. 147 (2000) 2081.
[11] P. Yu, J.A. Ritter, R.E. White, B.N. Popov, J. Electrochem. Soc. 147 (2000) 1280.
[12] B. Veeraraghavan, A. Durairajan, B. Haran, B. Popov, R. Guidotti, J. Electrochem. Soc. 149 (2002) A675.
[13] S. Kim, Y. Kadoma, H. Ikuta, Y. Uchimoto, M. Wakihara, Electrochem. Solid State Lett. 4 (2001) A109.
[14] C. Natarajan, H. Fujimoto, K. Tokuwasu, T. Kasuh, J. Power Sources 92 (2001) 187.
[15] J. Yang, J.O. Besenhard, M. Winter, Electrochem. Soc. Proc. 97–18 (1997) 350.